Anharmonic Oscillations, Dissipative Solitons and Non-Ohmic Supersonic Electric Transport

M.G. Velarde, W. Ebeling, and A.P. Chetverikov

Abstract We consider the Toda lattice with exponentially repulsive interactions between the units and view these units as Brownian elements capable of pumping energy from a surrounding heat bath or reservoir, and we show that solitons can be excited and maintained in the presence of dissipation. Then, we endow these Toda lattice units with electric charge, i.e., we make them positive ions and add free electrons to the system. We use this to show that, in the presence of an external electric field, following an instability of the base linear Ohm conduction state, the electromechanical Toda lattice is able to maintain a non-Ohmic soliton-driven supersonic electric current, and we then discuss its striking characteristics. Thus the lattice appears very much like a versatile neural transmission line.

1 Introduction

The soliton concept, and the coinage of the word soliton, originates from the work of Zabusky and Kruskal [1] (see also [2, 3, 4]). They dealt with the dynamics of one-dimensional (1D) anharmonic lattices and their (quasi) continuum approximation [5] provided by the Boussinesq–Korteweg-de Vries (BKdV) equation [6, 7]. That work followed research done by Fermi et al. [8] (see also [9]) who tried to understand equi-partition in a lattice by adding anharmonic forces. They used 1D lattices with 16, 32 and 64 units interacting with springs obeying x^2 and x^3 anharmonic

M.G. Velarde
Instituto Pluridisciplinar, Universidad Complutense de Madrid, Paseo Juan XXIII, 1, E-28040 Madrid, Spain, mgvelarde@pluri.ucm.es

W. Ebeling
Institut für Physik, Humboldt-Universität Berlin, Newtonstr. 15, D-12489 Berlin, Germany, ebeling@physik.hu-berlin.de

A.P. Chetverikov
Faculty of Physics, Chernychevsky State University, Astrakhanskaya 83, 410012 Saratov, Russia, chetverikovAP@info.sgu.ru

Velarde, M.G. et al.: *Anharmonic Oscillations, Dissipative Solitons and Non-Ohmic Supersonic Electric Transport.* Lect. Notes Phys. **751**, 321–335 (2008)
DOI 10.1007/978-3-540-78217-9_12

forces and another described by a nonlinear but "piecewise linear" function. The significant achievements of Visscher and collaborators are also worth mentioning. While trying to understand heat transfer, they used the Lennard-Jones potential [10] to explore the role of anharmonicity and of impurities (i.e., doping a given lattice with different masses, thus generating isotopically disordered lattices). More recently, Heeger, Schrieffer and collaborators have used solitons to explain the electrical conductivity of polymers [11]. Finally, we ought to highlight the work done by Toda (1967) on the lattice (which he invented) with a peculiar exponential interaction [12, 13], since here we build upon the results obtained by Toda. [N.B. We make no claim of completeness in the list of references offered here. For a thorough, albeit now a bit old, review of solitons in condensed matter, see Bishop et al. [14]; for an in-depth discussion of heat transfer see Toda [15].]

In one limit, the Toda interaction yields the hard rod/sphere impulsive force (a gas), while in another limit, it becomes a harmonic oscillator (the ideal solid lattice crystal). When the force is proportional to displacement or elongation (x), we have Hooke's law, and this defines the realm of linear oscillations (harmonic in Fourier space), or phonons in the quantum terminology. Through a suitable Taylor expansion, the Toda interaction provides the aforementioned x^2 and x^3 anharmonic forces beyond Hooke's law. Figure 1 illustrates Toda's interaction (with its exponential-repulsive and linear-attractive parts) relative to the Lennard-Jones and Morse interactions. As the latter is a combination of exponentials, both the Toda and Morse interactions are easy to implement electronically. The mechanical–electrical analogy has been fruitfully exploited by researchers [13, 16, 17, 18].

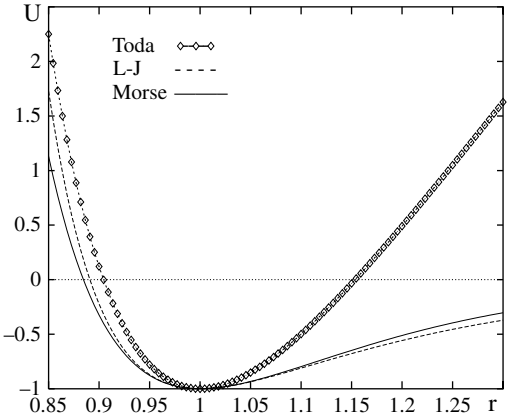

Fig. 1 Toda potential $(U = U^{\mathrm{T}} = \frac{a}{b}[\mathrm{e}^{-b\sigma(r-1)} - 1 + b\sigma(r-1)])$, Morse potential $(U = U^{\mathrm{M}} = \frac{a}{2b}[(\mathrm{e}^{-b\sigma(r-1)} - 1)^2 - 1])$ and Lennard-Jones potential $\left(U = U^{\text{L-J}} = U_0\left[\frac{1}{r^{12}} - \frac{1}{r^6} - 1\right]\right)$. In order to have all three minima of the potential functions at the same location, i.e., $(1, -1)$, we have suitably adjusted the free parameters, while keeping the same basic frequency; r is a suitably rescaled length quantity. It clearly appears that Toda's interaction captures the repulsive core in a good way, whereas its attractive part becomes unphysical for large values of the displacement. Both the Toda and Morse potentials are easily implemented with present-day electronics, as they contain exponentials

The concept of *dissipative* solitons extends the classical theory to non-conservative systems where energy (rather than being conserved) is pumped and dissipated in an appropriate balance, thus exciting and, eventually, sustaining a localized structure (or a periodic nonlinear wave) beyond an instability threshold [19, 20, 21]. The concept of *dissipative* solitons is also the natural generalization of a dynamical system consisting of maintained *dissipative* linear waves with an underlying *dissipative* harmonic oscillator [22, 23, 24, 25, 26, 27].

In this text, we limit ourselves entirely to one-dimensional (1D) lattice systems in classical (not quantum) mechanics. In Sect. 2, we recall how solitons (and nonlinear periodic cnoidal waves) appear in the Toda lattice and give a few other results needed in the subsequent sections of this chapter. Section 3 is devoted to a description of a first generalization of Toda's lattice, made by adding an energy pumping–dissipation balance. In Sects. 4 and 5, we add electric charges and we discuss the electric currents that our generalized driven-dissipative Toda lattice can exhibit in the presence of an external electric field. In particular, we discuss the recent striking discovery [28] of the onset and eventual sustenance of electron–soliton dynamic bound states (solectrons) and the "truth and consequences" that follow: a form of (purely classical) "high"-temperature supersonic current following a transition from the linear (Ohm–Drude) conduction state. Section 6 provides conclusions and suggestions for future research.

2 Solitons and Cnoidal Waves in a Toda Lattice

Let us consider a 1D lattice with Toda interactions between nearest-neighbor units (Fig. 1). Here, relative to the harmonic case, we replace Hooke's law by the force corresponding to

$$U_i^{\mathrm{T}}(r_i) = \frac{a}{b}\left[\exp(-br_i) - 1 + br_i\right]. \tag{1}$$

The relative mutual displacement between the mass i and the mass $i+1$ is $r_i = x_{i+1} - x_i - \sigma$. Then (in the infinite case), there is an exact solution of the corresponding dynamical system (the system is integrable), as found by Toda [12, 13]. As mentioned earlier, if we expand (1) in a Taylor series

$$U^{\mathrm{T}}(r) = \frac{ab}{2}\left(r^2 - \frac{b}{3}r^3 + \cdots\right), \tag{2}$$

for small values of the displacements, r_i, from equilibrium positions, we recover, to lowest-order, the harmonic oscillator. Subsequent terms in the series (r^3, r^4) reproduce the aforementioned interactions used by Fermi, Pasta and Ulam. Apart from an external periodic forcing term, these define the (asymmetric nonlinear) Helmholtz oscillator [29] and the (symmetric nonlinear) Duffing oscillator, respectively. We see from the expansion (2) that, for the Toda potential, the parameter ab controls the basic oscillation frequency and the parameter ab^2 controls the anharmonicity of the forces acting between the particles, so that b can be interpreted as the stiffness

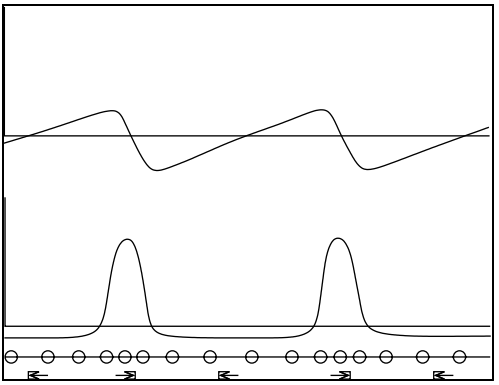

Fig. 2 Toda lattice. Lattice compressions (*bottom*) create solitons (pulse-like disturbances, solitary waves or periodic cnoidal wave peaks); momentum distribution along the lattice is shown at the top. Note that, taking into account the sign of the velocity (left to right motion), the former is the (negative) derivative of the latter

parameter of the springs. The solitary waves and (periodic) cnoidal waves found by Toda are the new "degrees of freedom" of the lattice, corresponding to Fourier modes in the linear approximation. For a uniform lattice $b_n = b(-\infty < n < \infty)$, the exact solutions are the cnoidal waves (Fig. 2)

$$\exp(-br_n) - 1 = m\frac{(2K\nu)^2}{ab}\left(\mathrm{dn}^2\left[2\left(\frac{n}{\lambda} \pm \nu t\right)K\right] - \frac{E(k)}{K(k)}\right), \tag{3}$$

where the wavelength λ and the frequency ν are related by the dispersion relation

$$\nu(\lambda) = \frac{\sqrt{\dfrac{ab}{m}}}{2K(k)\sqrt{\mathrm{sn}^{-2}(2K(k)/\lambda) - 1 + E(k)/K(k)}}. \tag{4}$$

Here $\mathrm{sn}(u)$ and $\mathrm{dn}(u)$ are elliptic functions with modulus k $(0 < k \leq 1)$. $K(k)$ and $E(k)$ are complete elliptic integrals [12, 13, 30].

When the modulus k is close to zero (i.e., for small values of the displacement), $E/K \simeq 1 - k^2/2$ and

$$r_n \simeq -\frac{\pi^2\nu^2k^2}{2ab^2}\cos 2\pi\left(\nu t \pm n/\lambda\right), \tag{5}$$

then the wave profile and dispersion of cnoidal waves in the Toda lattice are similar to those of harmonic (sinusoidal) waves in a linear lattice.

In the limit $k \to 1$, the cnoidal wave approaches a sequence of equally spaced delta functions. For $\lambda \approx K \to \infty (k \to 1)$, the result is a solitary wave

$$\exp\left(-b(r_{n+1} - r_n)\right) = 1 + \sinh^2(\chi)\,\mathrm{sech}^2\left(\chi n - t/\tau\right). \tag{6}$$

These "solitonic" excitations correspond to local compressions of the lattice with the characteristic compression time

$$\tau_{\mathrm{sol}} = (\omega \sinh\chi)^{-1} \tag{7}$$

and with a spatial "width" χ^{-1}. The energy of the soliton is related to this quantity by

$$\varepsilon_{\rm sol} = 2\frac{a}{b}(\sinh\chi\cosh\chi - \chi), \tag{8}$$

with σ taken as the unit of length. The soliton velocity is given by

$$v_{\rm sol} = \sigma\sqrt{\frac{ab}{m}}\frac{\sinh\chi}{\chi}, \tag{9}$$

which is supersonic, since the sound velocity in the corresponding linear lattice is $\sigma\sqrt{ab/m}$, with both velocities being given in common appropriate units [$\omega_0\sigma = \sigma\sqrt{ab/m}, \sigma = 1$ and even $\omega_0 = 1$ in most of the text]. Figure 2 illustrates how compressions create the solitonic peaks and the wave motion along the Toda lattice.

3 Self-Organization with an Input–Output Energy Balance

Driving, forcing and hence maintaining nonlinear oscillations in a Toda lattice can be achieved using the following Langevin equations:

$$\begin{aligned} \frac{\mathrm{d}}{\mathrm{d}t}x_i &= v_i, \\ m\frac{\mathrm{d}}{\mathrm{d}t}v_i + \frac{\partial U}{\partial x_i} &= F_i(v_i) + m\sqrt{2D}\,\xi_i(t), \end{aligned} \tag{10}$$

governing the evolution of the *i*th particle viewed as a Brownian element on the lattice. Here, the stochastic forces mimic embedding the system in a thermal bath or reservoir, from where the lattice units can pump energy in a kind of self-organization, obtaining order out of the noise. They have zero mean and are delta-correlated:

$$\begin{aligned} \langle\xi_i(t)\rangle &= 0, \\ \langle\xi_i(t)\xi_j(t)\rangle &= \delta_{ij}\delta(t'-t). \end{aligned}$$

Note that if we go back to the deterministic description ($D = 0$) and set $F_i = 0$, we get Newton's equations for the original Toda lattice [12, 13].

In order to introduce an input–output energy balance into the system, we define a force, F_i, including its *passive* and *active* components. Following Lord Rayleigh [22, 23], (an alternative is Van der Pol's approach [24]) we define a velocity-dependent friction force by

$$F(v) = F_0(v) + F_{\rm a}(v) = -m\gamma(v)\,v, \tag{11}$$

with

$$\gamma(v) = \gamma_0 + \gamma_{\rm a}(v), \tag{12}$$

where the first term, γ_0, describes the standard friction between the particles and the surrounding heat bath. For this *passive* friction, we assume the validity of the Einstein fluctuation–dissipation theorem [31, 32]. However, for simplicity, we assume that the *active* (non-equilibrium) part of the friction force, γ_a, does not fluctuate.

The balance for the total energy, ε, of the system (10) is

$$\frac{d\varepsilon}{dt} = -m\gamma_0 \sum_i v_i^2 - m \sum_i \gamma_a(v_i) v_i^2 + m\sqrt{2D} \sum_i v_i \xi_i. \tag{13}$$

Since $\gamma_0 > 0$, the sign of the active term, $\gamma_a(v)$, is crucial for the energy balance of our lattice if we wish to have a steady state ($d\varepsilon/dt = 0$). As noted earlier, this contribution to the friction function may describe *active* forces, which, due to their energy pumping effect, can drive the system away from equilibrium. Retaining Lord Rayleigh's law, we set

$$F_a(v) = -m\gamma_a(v)v = -m\left(-\hat{\gamma}_1 + \gamma_2 v^2\right) v;\ \hat{\gamma}_1,\ \gamma_2 > 0, \tag{14}$$

and hence, for $\hat{\gamma}_1 > \gamma_0$, we re-write the complete dissipative force as

$$F(v) = m\gamma_0 \left(\mu - v^2/v_d^2\right) v, \tag{15}$$

with

$$\mu = (\hat{\gamma}_1 - \gamma_0)/\gamma_0, \qquad v_d^2 = \gamma_0/\gamma_2. \tag{16}$$

Instead of the Rayleigh law, we may use a more refined law for the dissipative force by introducing the expression [31, 32]

$$\gamma_1 = -\gamma_0 \frac{\delta}{1 + v^2/\hat{v}_d^2}. \tag{17}$$

Then the total friction force acting on a particle may be represented as

$$F(v) = -m\gamma_0 \left[1 - \frac{\delta}{1 + v^2/\hat{v}_d^2}\right] v. \tag{18}$$

Note that (18) yields (15) for low velocity values when we replace $(\delta - 1)$ with μ and $\hat{v}_d^2$ with δv_d^2. For simplicity, we shall continue with (15).

The parameters μ and δ control the conversion of the energy taken up from the reservoir into kinetic energy. One or the other is the bifurcation parameter of our model. The values $\mu = -1$ and $\delta = 0$ correspond to equilibrium, the region $-1 < \mu < 0$, or $0 < \delta < 1$, stands for nonlinear *passive* friction and $\mu > 0$, or $\delta > 1$, corresponds to an *active* friction force. The bifurcation from one regime to the other occurs at $\mu = 0$, or $\delta = 1$. For the *passive* regime, the friction force vanishes at $v = 0$, which is the only attractor of the deterministic motion, i.e., with no noise, all particles come to rest at $v = 0$. For the *active* case, the point $v = 0$ becomes unstable, but we then have two additional zeros at

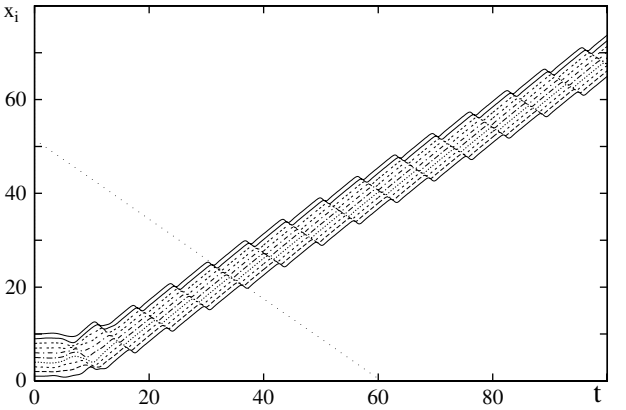

Fig. 3 Active Toda lattice. Trajectories (x, t) of 10 particles with added *active* Rayleigh friction force. Solitons (peaks of the cnoidal waves) appear traveling (*dotted line*) along the lattice in the direction which is opposite to that of the mean motions of the lattice particles. The single soliton is genuine solitary wave appearing in the lattice. It was obtained by suitably adjusting the randomly distributed initial velocities of the particles. The soliton velocity is given by the slope of the dotted line. Parameter values: $\omega_0 = 1$, $\sigma = 1$, $\gamma_0 = 0.8$, $\mu = 1$, $b = 1$ and $D = 0$

$$v = \pm v_0,\ v_0 = \hat{v}_\mathrm{d}\sqrt{\delta - 1} = \sqrt{\delta - 1},\ \text{as } \hat{v}_\mathrm{d} = 1 \text{ or } v_0 = v_\mathrm{d}\sqrt{\mu} = \sqrt{\mu},\ \text{as } v_\mathrm{d} = 1. \tag{19}$$

The two velocities, $\pm v_0$, are the new "attractors" of the free deterministic motion.

We look for a description with universality using dimensionless equations through an appropriate choice of scales. In the light of earlier comments, and for illustrative computational purposes, we set $m = 1$, $\sigma = 1$, and $\omega_0 = 1$. In Fig. 3, we show the result of a numerical integration of (10) for 10 lattice units without forcing and with no noise, but with an *active* friction force. The Toda lattice units are moving clockwise, while the excited soliton is moving counter-clockwise (as illustrated by the dotted line).

4 Electromechanical Toda Lattice

Let us consider the role of *dissipative* solitons in the *active* Toda lattice endowed with electric charges (ions and electrons). Hence, we now view the Toda lattice units as ions (charge $+e$ and mass m_i; $m_\mathrm{i} = m$) interacting with *free* electrons (charge $-e$ and mass $m_\mathrm{e} << m_\mathrm{i}$, $m_\mathrm{i} \approx 10^3 m_\mathrm{e}$; we expect no confusion regarding the subscripts "e" and "i", which here refer to electrons and ions, respectively). If we approximate the repulsion of the ions with a simple exponential law (see Fig. 1), then the 1D ion system on a lattice is equivalent to a 1D Toda lattice (1),

$$U(r_k) = \frac{m\omega_0^2}{b^2}\exp(-br_k) \tag{20}$$

(recall that $a/b = m\omega_0^2/b^2,\ \sigma = 1$). Thus, for small displacements, an ion moves in the harmonic potential of its nearest neighbors, while for larger values of the displacement, it feels a stiff (exponential) repulsion on each side. In principle, the stiffness, b, is a tunable parameter. Let us study the influence of the dynamics of the system on its electrical conductivity.

Let us place the N electrons at positions y_j (thus having electro-neutrality) and allow them to move freely in the non-uniform and, in general, time-dependent, electric field generated by the positive lattice particles (ions) located at lattice positions x_k. For simplicity, we describe the electron–ion interaction with a pseudo-potential with an appropriate cut-off [33]:

$$U_{\mathrm{e}}(y_j) = \sum_k \frac{(-e)e}{\sqrt{(y_j - x_k)^2 + h^2}}. \tag{21}$$

This potential avoids the pole (a Coulomb singularity) by introducing a cut-off at $U_{\min} = -e^2/h$; $h \approx \sigma/2$ is the cut-off distance and, as previously noted, σ is the equilibrium inter-ion mean distance. [N.B. Quantum mechanically, (21) is justified by the fact that, in a real solid, the ion core is a region of high electronic density and finite size, and so it can hardly be penetrated by a *free* electron.] Figure 4 illustrates, using suitable dimensionless quantities, the role of the cut-off, h, and of the compression of the Toda springs in the lattice.

To avoid Coulomb singularities in 1D or 2D geometry in (21), we consider the *free* electrons to be moving along the lattice in 3D. Accordingly, the electrons are able to move from one side of an ion to the other. Also, for simplicity, the interaction between electrons is neglected. Thus, with N ions placed at co-ordinates x_k, moving

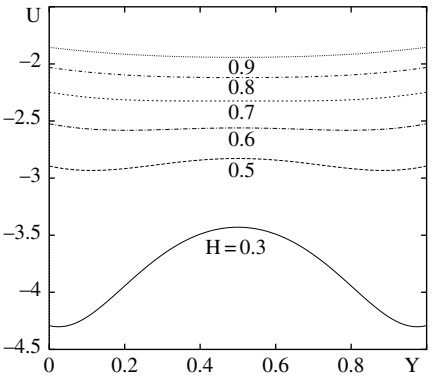

Fig. 4 Electromechanical Toda lattice. Pseudo-potential (21) experienced by an electron placed midway between two nearby ions. The graphs here appear in universal forms, since we use $H \equiv h/r, Y \equiv y/r, X \equiv x/r$, hence $x_1 = 0 \to X = 0, x_2 = r \to X = 1$ and $0 < y < r \to 0 < Y < 1$. Also, $U(Y)/e^2 = -\left[Y^2 + H^2\right]^{-1/2} - \left[(Y-1)^2 + H^2\right]^{-1/2}$. As H grows, either because h grows (cut-off length increases) or r decreases (compression increases), the maximum yields to a minimum midway between the two ions

on a lattice of length $L = N\sigma$, and in view of the evolution assumed for the ions (10), we now make use of Langevin dynamics for electrons, which are also taken to be Brownian elements:

$$\begin{aligned} \frac{\mathrm{d}}{\mathrm{d}t} y_j &= v_j, \\ m_\mathrm{e}\frac{\mathrm{d}v_j}{\mathrm{d}t} + \sum_k \frac{\partial U_\mathrm{e}(y_j, x_k)}{\partial y_j} &= -eE - m_\mathrm{e}\gamma_{\mathrm{e}0} v_j + m_\mathrm{e}\sqrt{2D_\mathrm{e}}\,\xi_j(t). \end{aligned} \tag{22}$$

We assume periodic boundary conditions. For further simplicity, we may, on occasion, consider just one electron located at a position y, rather than N (non-interacting) electrons at co-ordinates y_j. Note that the friction of the electrons is assumed to be purely *passive* (i.e., we have standard damping for all velocities). As for the ions (10), the stochastic force in (22) also models a surrounding heat bath (Gaussian white noise), but, following Einstein's relation [31, 32], temperatures need not be equal (as we disregard issues of thermal equilibrium). Note also that the friction force acting on the electron is small relative to that on the ions, $m_\mathrm{e}\gamma_{\mathrm{e}0} \ll m_\mathrm{i}\gamma_{\mathrm{i}0}$ (the subscript "0" denotes passive friction).

As we have now "ions" and "electrons", (1) must be replaced by

$$U = \sum_{k=1}^{N} [U_\mathrm{i}^\mathrm{T}(r_k) + U_\mathrm{e}(r_k)], \tag{23}$$

with $U_\mathrm{i}^\mathrm{T}(r_k)$ denoting the Toda exponential potential (1) and $U_\mathrm{e}(r_k)$ the electron–ion potential (21). The external electric field E also acts on the charge $e_\mathrm{i} = +e$ of the Toda particles (ions). Making the Rayleigh-like velocity-dependent force explicit, the Langevin equation in (10) becomes

$$m\frac{\mathrm{d}}{\mathrm{d}t} v_k + m\gamma_0 v_k + \frac{\partial U}{\partial x_k} = eE + F_\mathrm{a}(v_k) + m\sqrt{2D}\,\xi_k(t), \tag{24}$$

where k denotes the kth ion on the lattice ring. Our evolution problem is now the combined set of (22) and (24). These equations have been integrated by means of a fourth-order Runge–Kutta algorithm adapted for solving stochastic problems like the Langevin equation [34]. All computer runs begin with a state where the distances between ions are equal and their velocities are taken randomly from a normal distribution with amplitude v_in, $v_k(0) = v_\mathrm{in}\xi(k)$. Each electron is placed at rest, $v_j = 0$, midway between two ions. Heavy ions are not affected much by light electrons, and hence (free) electrons move on the background/landscape of the pseudo-potential profile created by the ions (Fig. 5). The integration step is chosen to correctly describe the fastest component of the process, viz. oscillations of electrons in a potential well. The parameters of both Toda and Coulomb potentials, the mass ratio and the particle charges are all held fixed in order to reduce the number of parameters of the problem. Thus, the damping rates, γ_0 and $\gamma_{\mathrm{e}0}$; the values of the parameters characterizing the driving forces, $F_\mathrm{a}(v_k)$; the initial velocity, v_in, chosen to select a

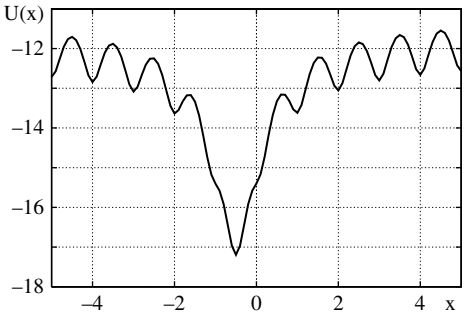

Fig. 5 Electromechanical Toda lattice. Snapshot of the effective potential/landscape acting on an electron moving in a lattice with a solitonic excitation which creates a locally deeper potential well. In a lattice which is sufficiently long, the solitonic (negative) peaks define a new periodicity (cnoidal waves) which is different from the other (quasi) harmonic one. Parameter values: $\sigma = 1$, $b = 1$ and $h/\sigma = 0.3$

solitonic mode; the value of the external field; and the electron temperature, T, are varied in the computer integrations.

5 From Ohm's Law to a Soliton-Mediated Supersonic Current

Due to the above-mentioned large difference in the masses of the charged particles, by far the major contribution to the current comes from the electrons moving on the nonlinear ion lattice. The current density (per unit length) of the electrons is obtained by taking average of the electron velocities. Hence, the electric current density (per unit length) is

$$j_{\mathrm{e}} = -n_{\mathrm{e}} e \sum_j \langle v_j^{\mathrm{e}} \rangle, \tag{25}$$

($n_{\mathrm{e}} = 1$ with 10 electrons and 10 ions). The average should be taken over sufficiently long trajectories. We are interested in the interaction of the electrons with the previously discussed (rather deep) solitonic excitations in the lattice (Fig. 5).

Before embarking on a study of electric currents, we study the effect of solitonic excitations generated through quenching by numerically finding the corresponding solutions of the coupled Langevin equations (22) and (24). Let us first discuss what happens if $E = F = 0$ in (24). The numerical integration was conducted by starting from a Gaussian distribution of the ion velocities, corresponding to a high-temperature Maxwellian as the initial condition. This temperature was of the order of 200–300 in units of $m\omega_0^2\sigma^2$, the energy of harmonic oscillations with amplitude σ (for clarity we make all variables and parameters explicit). At this rather high temperature, solitons should also be generated in addition to other elementary excitations. However, they are difficult to identify due to the seemingly chaotic motions

of the particles. Then, we quench to a temperature near zero. The solitons survive, since they have a longer lifetime than other excitations.

In another set of computer integrations, we combined quenching with active friction ($F \neq 0$) to overcome the dissipation. Again, the numerical integration started with a high-temperature initial condition, then, after quenching, the solitonic excitations were maintained by feeding in energy with Rayleigh's *active* friction force. In this case, and as noted earlier, the system develops solitons moving oppositely to the field. The electrons which are coupled to the charged Toda lattice units (ions) form rather stable dynamic bound states with the solitons (solectrons). For illustration, we take (unless otherwise specified) $\mu = 1$. Most of the time, the electrons will be located near local ion clusters, since they seek the deepest nearby minimum of the potential (see Fig. 4). Note that we have a dynamic process which does not lead to a static cluster, as the ions participating in the local compression are changing all the time. In other words, the electrons continually have new partners (a kind of promiscuity) in forming the bound states.

[N.B. An active Toda lattice (with Rayleigh's *active* friction force) with N particles possesses $(N+1)$ basic attractors. Of these, $(N-1)$ are oscillatory and two are non-oscillatory. (As a whole, the lattice moves to the right or left or clockwise/counter-clockwise in a lattice ring.) For N even, there is also an "optical" mode, corresponding to anti-phase oscillations. Here, we opt not to discuss this wealth of possibilities and hence, once more, refer the reader to recent publications on the subject [17, 18, 35].]

In Fig. 6, we show the evolution of 10 Toda lattice units (ions) creating 1 dissipative soliton which moves in the opposite direction and 10 *free*, non-interacting electrons. After a sufficient time interval, most of the electrons bind to the soliton, one after another, and move with a velocity which is approximately that of the

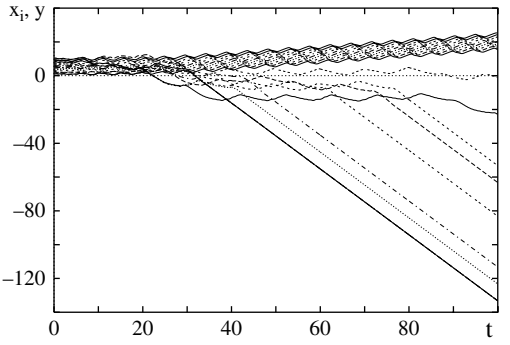

Fig. 6 Active electric Toda lattice. Trajectories are shown for 10 particles (ions) moving left to right, creating one fast dissipative soliton moving in the opposite direction, and for 10 electrons (ending, generally, as *sloped lines*) captured, one after another, by the soliton. Three electrons seem to be traveling together (*thicker sloped line*), while the 10th electron still moves almost freely (trajectory around $y = 0$). Parameter values: $h = 0.3$, $\mu = 0.25$, $\gamma_0 = \gamma_{e0} = 0.5$, $D = D_e = 0$ and $m/m_e = 10^3$. Unit time along abscissa: $t/\sqrt{5}$

soliton in a direction opposite to that of the ions. Needless to say, this is possible in the context of pure classical mechanics with the free non-interacting electron approximation that we have used here.

We have seen in the computer simulations that, when $\mu > 0$ for $E \neq 0$, the ions execute a slow drift following the direction of the external field. If the field strength is stronger than the decay imposed by the thermal fluctuations, then the electrons proceed in opposite direction. After a sufficient time interval, the ion compressions create solitonic excitations moving with the soliton velocity, v_{sol}, and opposite to the mean drift of the ions. As discussed in the earlier case, the electrons "like" the potential well formed by the local compression connected with the soliton (Fig. 5). After a while, the electrons are captured by the local compressions and move with the soliton velocity and opposite to the ion drift.

The magnitudes of both the electron and ion currents do not depend on the value of the external field over a wide range. Figure 7 shows both currents versus field strength. The scale, E_0, corresponds to the field imparting a velocity v_0 to an electron which is not interacting with the ions. It clearly appears that the stationary currents corresponding to the case of dissipative solitons are indeed stabilized, thanks to the *active* friction force that is due to energy pumping or, more precisely, to the input–output energy balance. At very low values of the field strength, we observe an apparent gap in the values for the current. In this narrow region, around zero, we could not obtain reliable data from the computer simulations. For very low electric field strengths, we cannot specify the running direction for solitons, and they may travel in either direction. On the other hand, intense field values do not allow electrons to be trapped easily by a potential well. In particular, at the upper boundary of the range, electrons are only captured by the soliton for a very limited domain of initial conditions for ions and electrons.

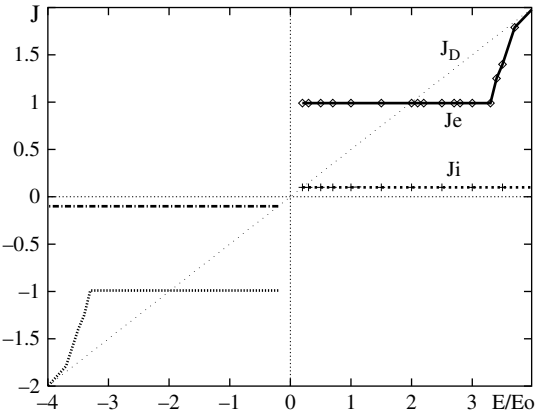

Fig. 7 Active electric Toda lattice. Current-field characteristics displaying the steady current densities (j_{D}, Ohm–Drude; j_{i}, ion current; and j_{e}, electron current). We see nonlinear current-field characteristics with a region of constant current. We observe an apparent gap in the values for the current at very small field values. Parameter values: $h = 0.3$, $\mu = 0.25$, $\gamma_0 = \gamma_{\mathrm{e}0} = 0.5$, $D = D_{\mathrm{e}} = 0$, $m/m_{\mathrm{e}} = 10^3$ and $b = 1$. E_0 is defined in the main text

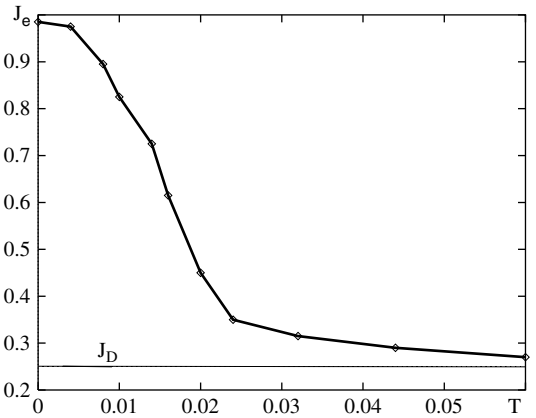

Fig. 8 Active electric Toda lattice. Current-temperature (electron noise) characteristics. The *solid line* (j_e, electron current) shows a significant increase as the temperature decreases and approaches the soliton range. The *horizontal straight dotted line* (ordinate 0.5) corresponds to the Ohm (Drude) current ($j_D = 0.25$). The value at $T = 0$ is the same as that of the plateau in Fig. 7. Parameter values: $b = 1$, $\mu = 0.25$, $h = 0.3$, $\gamma_0 = \gamma_{e0} = 0.5$, $T = D_e$, $D = 0$, $m/m_e = 10^3$ and $E/E_0 = 0.5$. E_0 is defined in the main text

Figure 8 illustrates the behavior of the electron current as a function of the temperature (electron noise). We see that, on lowering the temperature, the electron current driven by the solectrons grows significantly relative to the Ohm (Drude) current.

6 Final Remarks

The excitation of *dissipative* solitons in a Toda lattice has been discussed. In particular, we have studied the evolution of the lattice with added dissipation and "activity" in the form of energy pumping, following an idea put forward by Lord Rayleigh to maintain vibrations. We have considered the Toda lattice units as *active* Brownian elements. Then, we have studied the electrically charged (with ions and electrons) active Toda lattice and we have shown how the electric field triggers electric currents with striking properties. For such an active Toda lattice, we have shown how a (non-equilibrium) transition occurs beyond an instability threshold. This is from the linear Ohm (Drude) conduction (that can be viewed as defining a "disordered" state) to a form of "super-current" (that can be viewed as characterizing a more "ordered" state). The underlying mechanism of such a non-Ohmic supersonic current is the formation of electron–soliton dynamic bound states (solectrons) due to the role played by the compressions in the Toda springs. One of the most interesting properties of the phenomena studied here appears to be that, for a wide plateau, the strength of the external field is nearly irrelevant, and that what matters is its symmetry-breaking

role. On the other hand, it seems pertinent to point out that an electromechanical active Toda lattice can be seen as a versatile, two-speed neural-like cable. Recall that action potential propagation in axons, as in the case of the squid, proceeds at about 400 km/h [36]. This is the typical velocity of a super-critical ocean solitary wave and is equivalent to supersonic in the lattice studied here.

The study provided here is based on purely classical dynamics (i.e., no quantum mechanics is involved). Recent quantum mechanical calculations using the tight binding approximation for the electron–lattice interaction support the results reported in [37, 38, 39]. The results found, first reported in a 2005 letter [28], share common (formal) features with the experimental curves obtained in measurements of the characteristics of high-T superconductors [40, 41]. We are aware of pictures that look alike, yet refer to different objects. Hence, linking the predictions made using the purely classical analysis of a 1D Toda lattice model with data about real systems, or discussing any quantum effects, is beyond the scope of this discussion [42, 43].

Acknowledgments This research was, in part, supported by the EU under Grant SPARK.

References

1. N.J. Zabusky and M.D. Kruskal, Phys. Rev. Lett. **15**, 57 (1965).
2. A.C. Scott, F.Y.F. Chu and D.W. McLaughlin, Proc. IEEE **61**, 1443 (1973).
3. A.C. Scott, *Nonlinear Science: Emergence & Dynamics of Coherent Structures*, 2nd edn (Oxford University Press, New York, 2003).
4. N.J. Zabusky, Chaos **15**, 015102 (2005).
5. C.I. Christov, G.A. Maugin and M.G.Velarde, Phys. Rev. E **54**, 3621 (1996).
6. J.V. Boussinesq, Mém. présentés par divers savants à l'Acad. Sci. Inst. France (Paris) **23**, 1 (1877). J.V. Boussinesq, Mém. présentés par dívers savants à l'Acad. Sci. Inst. France (Paris) **24**, No. 2, 1 (1978).
7. D.J. Korteweg and G. de Vries, Phil. Mag. **39**, 442 (1895).
8. E. Fermi, J.R. Pasta and S.M. Ulam, *Studies of Nonlinear Problems* (Los Alamos Nat. Lab. Report LA-1940, 1955); Reprinted in *Collected Papers of Enrico Fermi*, (Univ. Chicago Press, Chicago, 1965) pp. 978–988.
9. G.P. Berman and F.M. Izrailev, Chaos **15**, 015104 (2005).
10. D.N. Payton III, M. Rich and W.M. Visscher, Phys. Rev **160**, 706 (1967).
11. A.J. Heeger, S. Kivelson, J.R. Schrieffer and W.P. Su, Rev. Mod. Phys. **60**, 781 (1988) (and references therein).
12. M. Toda, *Theory of Nonlinear Lattices*, 2nd edn (Springer-Verlag, New York, 1989a).
13. M. Toda, *Nonlinear Waves and Solitons* (KTK Scientific Publishers, Tokyo, 1989b).
14. A.R. Bishop, J.A. Krumhansl and S.E. Trullinger, Physica D **1**, 1 (1980).
15. M. Toda, Phys. Scripta **20**, 424 (1979).
16. M. Remoissenet, *Waves Called Solitons*, 3rd edn (Springer, Berlin, 1999).
17. V.A. Makarov, E. del Rio, W. Ebeling and M.G. Velarde, Phys. Rev. E **64**, 036601 (2001).
18. E. del Rio, V.A. Makarov, M.G. Velarde and W. Ebeling, Phys. Rev. E **67**, 056208 (2003).
19. C.I. Christov and M.G. Velarde, Physica D **86**, 323 (1995).
20. A.A. Nepomnyashchy, M.G. Velarde and P. Colinet, *Interfacial Phenomena and Convection* (CRC-Chapman & Hall, London, 2002), Chapter 5.

21. V.I. Nekorkin and M.G. Velarde, *Synergetic Phenomena in Active Lattices. Patterns, Waves, Solitons, Chaos* (Springer, Berlin, 2002).
22. J.W. Strutt (Lord Rayleigh), Phil. Mag. **15**, 229 (1883).
23. J.W. Strutt (Lord Rayleigh), *The Theory of Sound*, (original, 1894, reprinted by Dover, New York, 1945), vol. I, Sect. 68a.
24. B. Van der Pol, Phil. Mag. **2**, Ser. 7, 978 (1926). B. Van der Pol, Phil. Mag. **3**, Ser. 7, 65 (1927).
25. M.G. Velarde and X.-L. Chu, Phys. Lett. A **131**, 430 (1988).
26. X.-L. Chu and M.G. Velarde, Il Nuovo Cimento D **11**, 709 (1989).
27. M.G. Velarde, Benard layers, overstability and waves. In *Dynamics of Spatio-Temporal Cellular Structures-Henri Benard Centenary Review*, (Springer, New York, 2006, Springer Tracts in Modern Physics), Vol. 207, pp. 129–145.
28. M.G. Velarde, W. Ebeling and A.P. Chetverikov, Int. J. Bifurcat. Chaos **15**, 245 (2005).
29. E. del Rio, A. Rodriguez-Lozano and M.G. Velarde, Rev. Sci. Instrum. **63**, 4208 (1992).
30. M. Abramowitz and I.A. Stegun (eds.), *Handbook of Mathematical Functions, with Formulas, Graphs, and Mathematical Tables*, (Dover, New York, 1965).
31. F. Schweitzer: *Brownian Agents and Active Particles. Collective Dynamics in the Natural and Social Sciences* (Springer, Berlin, 2003).
32. W. Ebeling and I.M. Sokolov, *Statistical Thermodynamics and Stochastic Theory of Nonequilibrium Systems*, (World Scientific, Singapore, 2005).
33. V. Heine, M.L. Cohen and D. Weaire, *The Pseudopotential Concept*, (Academic Press, New York, 1970).
34. A.P. Chetverikov and J. Dunkel, Eur. Phys. J. B **35**, 239 (2003).
35. V.A. Makarov, M.G. Velarde, A.P. Chetverikov and W. Ebeling, Phys. Rev. E **73**, 066626 (2006).
36. J. Cronin, *Mathematical Aspects of Hodgkin-Huxley Neural Theory*, (Cambridge University Press, Cambridge, 1987).
37. M.G. Velarde, W. Ebeling, D. Hennig, and C. Neissner, Int. J. Bifurcat. Chaos **16**, 1035 (2006).
38. D. Hennig, C. Neissner, M.G. Velarde and W. Ebeling, Phys. Rev. B **73**, 024306 (2006).
39. A.P. Chetverikov, W. Ebeling, G. Röpke and M.G. Velarde, Contrib. Plasma Phys. **47**, 465 (2007).
40. P. Chaudhari, J. Mannhart, D. Dimos, C.C. Tsuei, J. Chi, M.M. Oprysko and M. Scheuermann, Phys. Rev. Lett. **60**, 1653 (1988).
41. J. Mannhart, P. Chaudhari, D. Dimos, C.C. Tsuei and T.R. McGuire, Phys. Rev. Lett. **61**, 2476 (1988).
42. D. Hennig, A.P. Chetverikov, M.G. Velarde and W. Ebeling, Phys. Rev. E **76**, 046602 (2007).
43. M.G. Velarde, W. Ebeling, A.P. Chetverikov and D. Hennig, Int. J. Bifurcat. Chaos **18**, 521 (2008).